KRZYSZTOF LUDWINEK*

SOME ASPECTS OF INDUCTANCE DISTRIBUTIONS MODELING IN *dq*0-AXES AND DAMPING CIRCUITS ON THE ROTOR OF A SALIENT POLE SYNCHRONOUS GENERATOR

WYBRANE PROBLEMY MODELOWANIA ROZKŁADU INDUKCYJNOŚCI W OSI *dq*0 I OBWODÓW TŁUMIĄCYCH WIRNIKA GENERATORA SYNCHRONICZNEGO JAWNOBIEGUNOWEGO

Abstract

This paper concerns a salient pole synchronous generator with damping bars on the rotor, and presents a comparison of the distribution of self and mutual inductances in the stator natural reference frame *abc* for a linear and a nonlinear circuital model, as well as in the rotor reference frame *dq*0. Moreover, this paper shows a proposed method of modeling the damping circuits on the rotor of a salient pole synchronous generator. An experimental verification of the registered induced voltage in the damping bars on the rotor is presented.

Keywords: *synchronous generator*, *inductance distributions*, *damping circuits*

Streszczenie

W niniejszym artykule przedstawiono – dla liniowego i nieliniowego modelu obwodowego generatora synchronicznego jawnobiegunowego z prętami tłumiącymi na wirniku – porównanie rozkładów indukcyjności własnych i wzajemnych w naturalnym układzie odniesienia *abc* związanym ze stojanem oraz w układzie odniesienia *dq*0 związanym z wirnikiem. Ponadto artykuł zawiera propozycję modelowania obwodów klatki tłumiącej wirnika generatora synchronicznego jawnobiegunowego. Opisane w nim też badanie eksperymentalne zarejestrowanych indukowanych napięć w prętach tłumiących wirnika.

Słowa kluczowe: *generator synchroniczny*, *rozkłady indukcyjności*, *obwody tłumiące*

* Ph.D. Eng. Krzysztof Ludwinek, Department of Industrial Electrical Engineering and Automatics, Kielce University of Technology.

1. Introduction

The most important aspect in simulations of electromagnetic properties of a synchronous generator and a squirrel cage induction motor using a circuital model are choosing suitable reference frames and the presence of damping bars (the most frequently on the rotor) [1–7]. If the self and mutual inductances of the stator windings contain only the constant component and the same magnitude of the 2nd harmonic, the simulation studies of synchronous generators using circuital models in the rotor reference frame $dq0$ are very popular due to constant self and mutual inductance distributions [1, 7]. The circuital models in $dq0$-axes are obtained using Park's transformation of the models in the stator natural reference frame. The inductance distributions in the $dq0$-axes for the magnetic core linearity can be expressed as [8]:

$$\mathbf{L}_{dq}(\theta) = \mathbf{B}(\theta)\mathbf{L}_s(\theta)\mathbf{B}^{-1}(\theta) \tag{1}$$

where:
   $d, q, 0$ – the winding in dices in the dq-axes and zero-sequence,
   θ – electrical angle of the rotor position,
   $\mathbf{L}_{dq0}$ – the matrix of self and mutual inductance distributions in the $dq0$-axes,
   $\mathbf{L}_s$ – the matrix of self and mutual inductance distributions of stator winding,
   $\mathbf{B}, \mathbf{B}^{-1}$ – matrixes of transformation and inverse transformation.

In expression (1) the inductance matrix $\mathbf{L}_{dq0}(\theta)$ in the $dq0$-axes can be formulated as [7]:

$$\mathbf{L}_{dq0}(\theta) = \begin{bmatrix} L_d(\theta) & L_{dq}(\theta) & L_{d0}(\theta) \\ L_{qd}(\theta) & L_q(\theta) & L_{q0}(\theta) \\ L_{0d}(\theta) & L_{0q}(\theta) & L_0(\theta) \end{bmatrix} \tag{2}$$

where:
   L_d, L_q, L_0 – self inductances in the $dq0$-axes,
   $L_{dq}, L_{qd}, L_{d0}, L_{0d}, L_{q0}, L_{0q}$ – mutual inductances in the $dq0$-axes.

Generally, in the stator and the rotor natural reference frame, the matrix of self and mutual inductances of synchronous generators $\mathbf{L}_{sfr}(\theta)$ (for magnetic core linearity) as a function of the electrical angle of the rotor position θ can be defined as [1–4, 7]:

$$\mathbf{L}_{sfr}(\theta) = \left[\begin{array}{c|c} \mathbf{L}_s(\theta)| & \mathbf{L}_{sr}(\theta) \\ \hline \mathbf{L}_{rs}(\theta)| & \mathbf{L}_r(\theta) \end{array} \right] \tag{3}$$

where:
   θ – electrical angle of the rotor position $\theta = \theta_m p$,
   θ_m – mechanical angle of the rotor position,
   p – the number of pole pairs,
   $\mathbf{L}_s$ – matrix of self and mutual inductance distributions of stator windings,
   $\mathbf{L}_{sr}, \mathbf{L}_{rs}$ – matrixes of mutual inductance distributions of stator and rotor windings,
   $\mathbf{L}_r$ – matrix of self and mutual inductance distribution of rotor windings.

Most often, the inductances in expression (3) can be calculated as follows:
– In an experimental way, e.g. Standstill Frequency Response Test (SSFR), Pseudo-
-Random Binary Sequence (PRBS) [9, 10] etc.,
– With the use of programs based on the finite element method using commercial
software, such as Maxwell, Flux, Opera etc, or using widely available Finite Element
Method Magnetics (FEMM) software, or using the edge element method [11–16],
– By means of one's own programs developed in LabView, Matlab/Simulink, etc.
[3, 10],
– By the combination of electromagnetic field equations and differential equations using
the commercial software (Maxwell, Flux, Opera etc.) [12],
– In ananalytical way [1, 17, 18].

Generally, for a non-uniform air gap on the stator and rotor side (for linear cases), the self and mutual inductances $L_{mn(v)}$ in relationship (1) are a function of the electrical rotor position angle θ, and for the v-th spatial harmonic inductance they can be described by means of a triple Fourier series [1]:

$$L_{mn(v)} = \sum_{v} \sum_{r} \sum_{s} L_{sr(v)}^{mn} e^{jv(\alpha_m - \alpha_n)} e^{jr\alpha_m} e^{js\theta} \tag{4}$$

where:

m, n – the index of arbitrary stator and rotor windings,
α_m – the angle between the individual stator winding magnetic axes and the stator reference axis,
α_n – the angle between the individual rotor winding magnetic axis and the rotor reference axis,
r, s – indices depending on the harmonic orders of the permeance function, representing the geometry of a rotor and stator air gap sides.

In this paper, the self and mutual inductances for the distributed stator windings and rotor damping bars are determined using the FEMM program in 2D [16]. In the case of 2D programs, the end leakage inductance should be calculated using, for example, the analytical technique [19–20].

Moreover, in this paper, for the linear circuit model, the influence of the higher harmonic contents of the $\mathbf{L}_s(\theta)$ in the stator natural reference frame *abc*, as well as $\mathbf{L}_{dq0}(\theta)$ in the rotor reference frame *dq*0 are presented. The $\mathbf{L}_{sr}(\theta)$, $\mathbf{L}_{rs}(\theta)$ and $\mathbf{L}_r(\theta)$ matrices (3) are not taken into account in this paper.

In the circuital modeling of a synchronous generator, apart from choosing suitable reference frames, another serious problem is the presence of the damping circuits [4, 5, 8, 11, 21, 22]. As shown in [23, 24] due to the presence of the damping circuits on the rotor, the *THDu* (total harmonic distortion) in induced stator voltage in the no-load state is higher than in the case of the rotor without the damping circuits. This is due to the components $\mathbf{L}_{sr} d\mathbf{i}_r/dt$ in a circuital model, where, the current derivative $d\mathbf{i}_r/dt$ in some damping bars of the examined 5.5 kVA salient pole synchronous generator has a value of almost 20 kA/s [23]. The most important aspect of computing the damper circuit in a synchronous and a squirrel cage motor is to obtain the current distribution in damping bars. Classical calculation of current distribution in damping bars on the rotor is usually performed analytically [1, 3–6,

8, 24]. This paper shows a proposed method of modeling the damping circuits on the rotor of a salient pole synchronous generator on the example of 10 damping bars on the rotor.

In this paper, the self and mutual inductances $\mathbf{L}_s(\theta)$ in expression (3) and $\mathbf{L}_{dq0}(\theta)$ in expression (2) are carried out on the basis of the real construction data of a salient pole synchronous generator rated: $S_N = 5.5$ kVA; $U_N = 400$ V (Y); $n_N = 3000$ rpm; $I_N = 7.9$ A; $\cos\varphi_N = 0.8$; $Q_s = 24$ (number of stator slots) factory single-layer winding; 10-damping bars shorted by two ring segments. Moreover, the number of pole pairs $p = 1$, a rotor with and without the skew is taken into account (the factory rotor skew α_q is equal to 15° and is equal to stator slot pitch). Calculating the self and mutual inductance distributions (as a function of the stator currents and electrical rotor position angle θ) are carried out in the FEMM 2D software and a linear and nonlinear magnetic circuit are taken into account. In the FEMM 2D software, the skew effect is obtained by subdividing the active rotor length into 5 skewed axial slides along the axial length. An inductance distribution with the rotor skew L_{mns} is calculated as [7]:

$$L_{mns} = \frac{1}{\alpha_q} \int_{\theta-\frac{\alpha_q}{2}}^{\theta+\frac{\alpha_q}{2}} L_{mn}\partial\theta \tag{5}$$

where:

α_q — an electrical rotor skew,
L_{mns}, L_{mn} — the inductance with and without a rotor skew, respectively.

A method of determining the self and mutual inductance distributions in the 2D FEMM program is detailed presented in [23, 25].

2. Stator winding self and mutual inductances

Figure 1 presents magnetic flux distribution lines of the examined 5.5 kVA nonlinear salient pole synchronous generator with 10 damping bars (5 bars per pole). In Figure 1, an example of slot leakage flux which penetrates the rotor pole pieces is shown. In Figure 1,
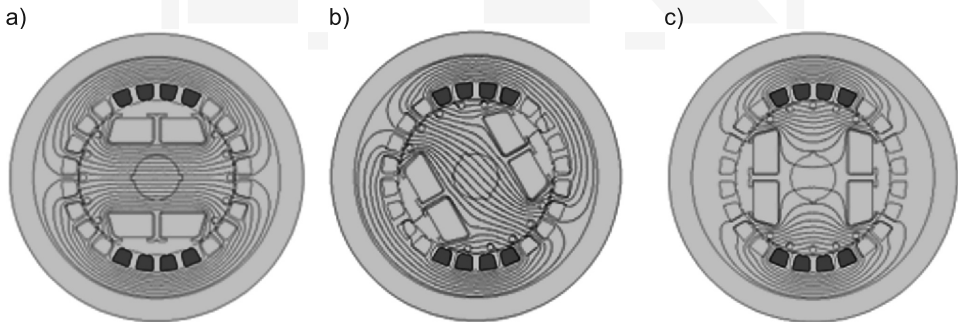
Fig. 1. Influence of the rotor position on magnetic field distribution and slot leakage flux: a) $\theta = 0$ deg, b) $\theta = 55$ deg, c) $\theta = 90$ deg

the total field on the rotor position is presented. At $\theta = 90°$, the total field can also be observed, but in q axis.

The magnetic field distribution, shown in Fig. 1, is obtained from stator current flowing in the phase winding a (in Fig. 1– four upper and four lower slots). Figure 2a–d shows the distributed stator winding self and mutual inductances for the linear and nonlinear model L_a, L_{an} (without the skew), L_{as}, L_{asn} (with the skew) and L_{ab}, L_{abn} (without the skew), L_{abs}, L_{absn} (with the skew) versus the electrical angular position of the rotor for the nominal stator current $I_N = 7.9$ A.
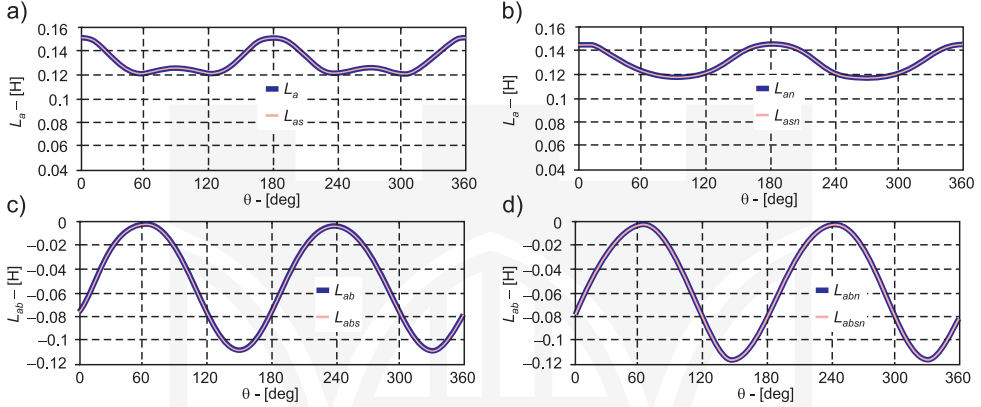

Fig. 2. Comparison of distribution of the stator winding self and mutual inductances versus the angular position of the rotor with the skew (index s) and without the skew for linear and nonlinear model: a) L_{as}, L_a, b) L_{asn}, L_{an}, c) L_{abs}, L_{ab}, d) L_{absn}, L_{abn}

In Figure 3, the comparison of distribution of the stator winding self and mutual inductances (Fig. 2) due to Fourier analysis is presented.
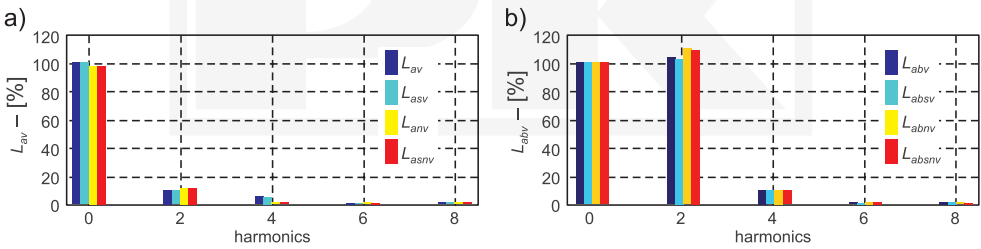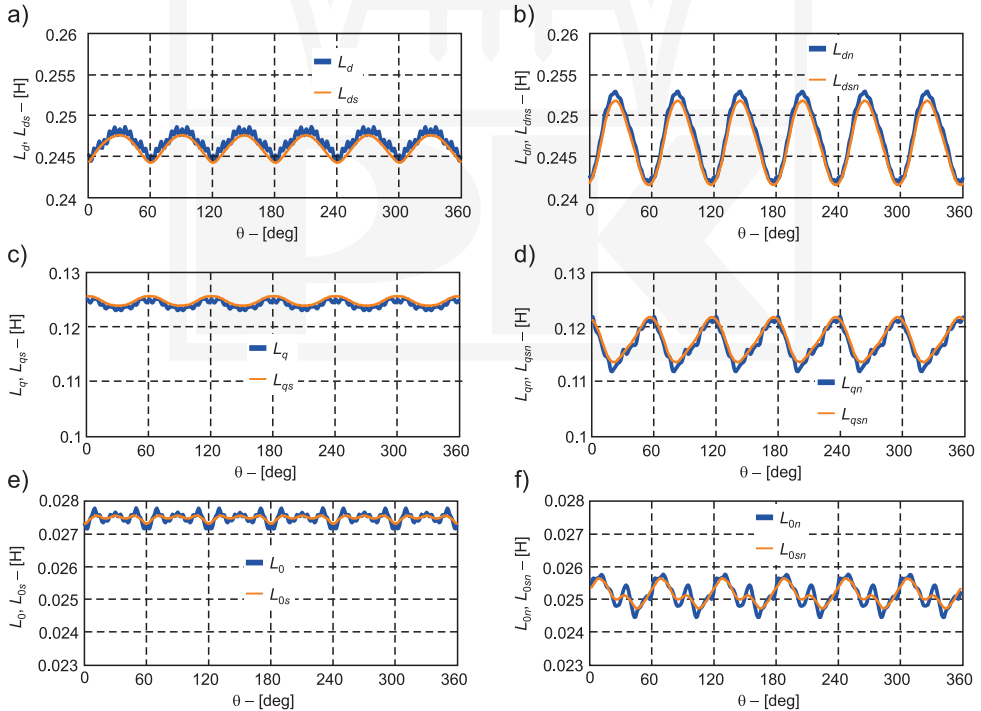

Fig. 3. Comparison of distribution of the stator winding self and mutual inductances with and without the rotor skew: a) L_{as}, L_a for linear model, L_{asn}, L_{an} for nonlinear model, b) L_{abs}, L_{ab} for linear model, L_{absn}, L_{abn} for nonlinear model

From presented the self and mutual stator inductance distributions (Fig. 2) and the higher harmonic contents (Fig. 3), it can be concluded that one rotation of the rotor makes the two--fold change of the magnetic permeability in the d and q axes and introduces a significant

inductance variation in each stator winding. Moreover, the value of the leakage flux varies depending on the electrical angular position of the rotor. This results in the largest participation of even harmonics in the distribution of the mutual stator inductances, among which, the most significant is the 2nd harmonic significantly greater than the second harmonic magnitude of the self-inductance (of the stator winding). A large participation of the second harmonic magnitude is the result of the participation of the slot leakage flux which even penetrates the rotor pole pieces [19]. The amplitudes of the higher harmonic components lying near the fundamental component due to the rotor skew (α_q = 15 deg) and are only reduced to a small extent. The reduction of spatial harmonic distribution of the self and mutual inductances by the skew of the rotor for the examined synchronous generator is presented in detail in [25].

3. A distribution of the self and mutual stator inductances in the *dq*0-axes

Figure 4 shows a comparison of the distribution of the self and mutual inductances in *dq*0-axes for the linear and nonlinear model with and without the rotor skew versus the electrical angular rotor position. The distributions are calculated on the basis of relationships (1) and (3) whilst taking into account the self and mutual stator inductances (Fig. 2). The self and mutual inductances in the *dq*0-axes after Park's transformation of the matrix $\mathbf{L}_s(\theta, \mathbf{i}_s)$ (3) are presented in detail in the paper [7].
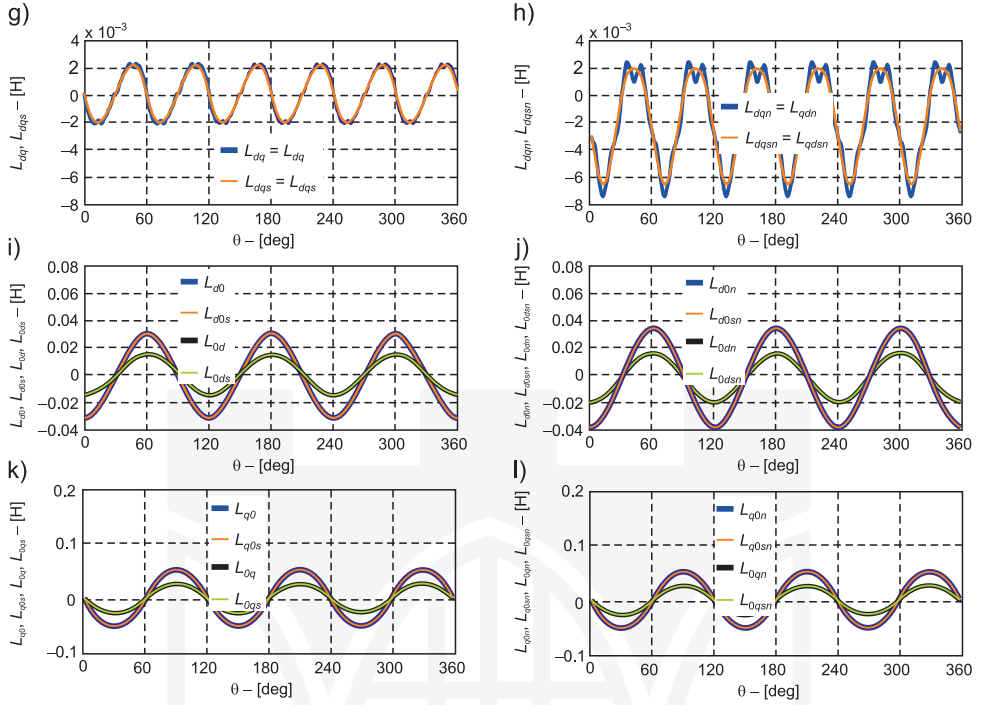
Fig. 4. Comparison of the self and mutual inductance distributions in the $dq0$-axes with and without the skew for linear and nonlinear model: a) L_d and L_{ds}, b) L_{dn} and L_{dsn}, c) L_q and L_{qs}, d) L_{qn} and L_{qsn}, e) L_0 and L_{0s}, f) L_{0n} and L_{0sn}, g) $L_{dq}(L_{qd})$ and $L_{dqs}(L_{qds})$, h) $L_{dqn}(L_{qdn})$ and $L_{dqsn}(L_{qdsn})$, i) L_{d0}, L_{0d} and L_{d0s}, L_{0ds}, j) L_{d0n}, L_{0dn} and L_{d0sn}, L_{0dsn}, k) L_{q0}, L_{0q} and L_{q0s}, L_{0qs}, l) L_{q0}, L_{0q} and L_{q0s}, L_{0qs}

If the self and mutual inductances of the stator windings contain the constant component, the 2nd and the higher harmonics, than the self and mutual inductances in the $dq0$-axes depend on the rotor position angle (Fig. 4). In the self inductance distributions, L_d, L_q, L_0 and in the mutual ones L_{dq} and L_{qd} dominate 6th harmonic. In other mutual inductance distributions, L_{d0}, L_{0d} and L_{q0}, L_{0q} dominate 3rd harmonic.

4. Modeling the damping circuits on the rotor

In dynamic states, the electromagnetic properties of a salient pole synchronous generator depend on the presence of the damping circuits [8, 11, 21, 22]. On the one hand, the damping circuits allow for shortening many transients' stages, e.g. the hunting, reducing higher harmonics in the field winding current [6, 22]. On the other hand, the damping circuits, due to higher harmonic currents, have an influence upon increasing higher harmonic contents in induced stator phase voltages (and armature currents in load states) in synchronous generator [6, 23]. The way of representation elements of damping circuits in circuital model has an

influence on the induced voltage waveforms in the stator windings, in the field winding and in the damping bars [11, 12, 21, 23]. There are many ways to obtain the parameters of the damping circuits, e.g. in an experimental and an analytical way or FEM methods [11, 12, 21]. The classical calculation of currents in the damping circuits on the rotor of a synchronous generator and an induction motor is usually performed analytically [1, 3, 21, 24]. In Figure 5, equivalent circuit parameters of damping circuits for the salient pole synchronous generator in the rotor natural reference frame is presented [5]. The damping circuit consists of ten damping bars and elements of end rings.
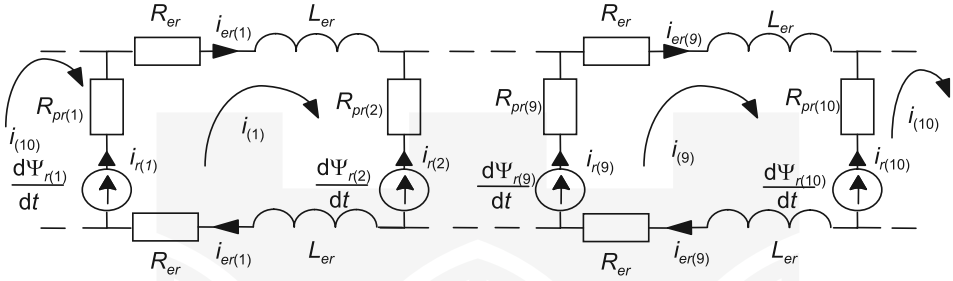

Fig. 5. Equivalent circuit parameters of ten damping circuits

Shown in Figure 1, each element in the circuits denotes [5]:

- in the k-th damping bar: R_{pr} resistive element and $e_{r(k)} = \mathrm{d}\Psi_{r(k)}/\mathrm{d}t$ induced voltage in the inductance lying in the pole piece in the area of the main flux,
- in the k-th segment of short circuital ring element: R_{er} resistive and L_{er} leakage inductance lying in the area outside the main flux. These elements for 2D models are calculated in an analytical way.

The inductances and resistances of the damping circuits (Fig. 5) can be described by means of the methods of circuit theory in the following forms [1, 3, 5, 24]:

$$\mathbf{R}_{rr} = \begin{bmatrix} 2(R_{pr}+R_{er}) & -R_{er} & 0 & 0 & \dots & -R_{er} \\ -R_{er} & 2(R_{pr}+R_{er}) & -R_{er} & 0 & \dots & 0 \\ 0 & -R_{er} & 2(R_{pr}+R_{er}) & -R_{er} & \dots & 0 \\ \dots & \dots & \dots & \dots & \dots & 0 \\ -R_{er} & 0 & 0 & 0 & -R_{er} & 2(R_{pr}+R_{er}) \end{bmatrix} \quad (6)$$

$$\mathbf{L}_{\sigma rr} = \begin{bmatrix} 2(L_{\sigma pr}+L_{er}) & -L_{er} & 0 & 0 & \dots & -L_{er} \\ -L_{\sigma er} & 2(L_{\sigma pr}+L_{er}) & -L_{er} & 0 & \dots & 0 \\ 0 & -L_{er} & 2(L_{\sigma pr}+L_{er}) & -L_{er} & \dots & 0 \\ \dots & \dots & \dots & \dots & \dots & 0 \\ -L_{er} & 0 & 0 & 0 & -L_{er} & 2(L_{\sigma pr}+L_{er}) \end{bmatrix} \quad (7)$$

$$\mathbf{L}_{rr}(\theta,\mathbf{i}_r) = \begin{bmatrix} L_{r(1)}(\theta,\mathbf{i}_r) & L_{r(1,2)}(\theta,\mathbf{i}_r) & L_{r(1,3)}(\theta,\mathbf{i}_r) & L_{r(1,4)}(\theta,\mathbf{i}_r) & \dots & L_{r(1,10)}(\theta,\mathbf{i}_r) \\ L_{r(2,1)}(\theta,\mathbf{i}_r) & L_{r(2)}(\theta,\mathbf{i}_r) & L_{r(2,3)}(\theta,\mathbf{i}_r) & L_{r(2,4)}(\theta,\mathbf{i}_r) & \dots & L_{r(2,10)}(\theta,\mathbf{i}_r) \\ L_{r(3,1)}(\theta,\mathbf{i}_r) & L_{r(3,2)}(\theta,\mathbf{i}_r) & L_{r(3)}(\theta,\mathbf{i}_r) & L_{r(3,4)}(\theta,\mathbf{i}_r) & \dots & L_{r(3,10)}(\theta,\mathbf{i}_r) \\ \dots & \dots & \dots & \dots & \dots & \dots \\ L_{r(10,1)}(\theta,\mathbf{i}_r) & L_{r(10,2)}(\theta,\mathbf{i}_r) & L_{r(10,3)}(\theta,\mathbf{i}_r) & L_{r(10,4)}(\theta,\mathbf{i}_r) & \dots & L_{r(1,10)}(\theta,\mathbf{i}_r) \end{bmatrix}$$

(8)

where:

$L_{r(k)}$, $L_{r(k,l)}$ – self and mutual inductances in the k-th damping circuits,
L_{er} – leakage inductance of end ring elements,
$L_{\sigma pr}$ – leakage inductance of damping circuits,
k,l – indexes in the k-th and l-th damping circuits,
$\mathbf{R}_{rr}$ – matrix of resistive of damping bars and shorted ring elements,
$\mathbf{L}_{\sigma rr}$ – matrix of leakage inductance,
$\mathbf{L}_{rr}$ – matrix of self and mutual inductances of damping circuits.
$\mathbf{i}_r$ – matrix of damping circuit currents $[i_{r(1)}, \dots, i_{r(k)}]^T$.

Elements R_{er} and L_{er} of the circuital ring segments (shown in Fig. 5) can be reduced to another form, creating a circuit diagram of the damping cage as shown in Fig. 6 [5]. As shown in the paper, the self and mutual inductance distributions in the $dq0$-axes are dependent on the angle position of the rotor. Moreover, the Park's transformation of the higher harmonics of the stator self and mutual inductance distributions to the $dq0$-axes does not eliminate the influence of the rotor position angle and, in simulations only, introduces additional unnecessary calculations [7]. Hence, in simulations of a salient pole synchronous
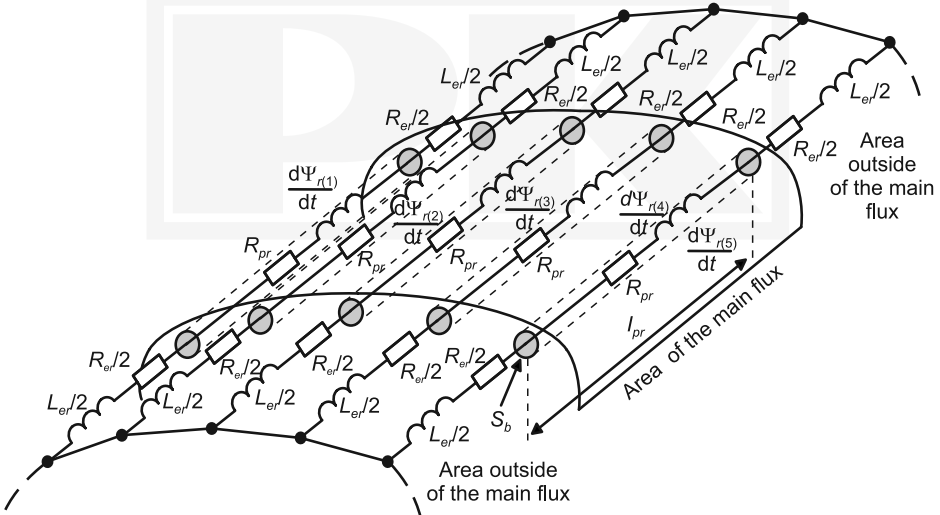

Fig. 6. Equivalent circuit parameters of damping circuits with elements lying
with area of main flux and area outside of the main flux

generator, the induced phase stator voltages u_a, u_b and u_c and stator currents i_a, i_b and i_c are easier to carry out with a circuital model in the stator and rotor natural reference frame.

Figure 7 shows the equivalent circuit parameters of a synchronous generator in a no--load state in the stator and rotor natural reference frame. The equivalent circuit parameters represent the stator windings, the field winding and shorted equivalent 5-damping bars per pole. Equivalent resistances $R_{r(k)}$ for $k = \{1, 2, \ldots 10\}$ damping bars and equivalent leakage inductances L'_{er} can be expressed as [5]:

$$R_{r(k)} = R_{pr(k)} + \frac{R_{er(k)}}{2(\sin \alpha_{Q_{r(k)}})^2} = R_{pr}(k) + R'_{er(k)} \quad \text{and} \quad L'_{er(k)} = \frac{L_{er(k)}}{2(\sin \alpha_{Q_{r(k)}})^2} \tag{9}$$

where:

$\alpha_{Q_{r(k)}}$ –   is the angle between the equivalent k-th rotor damping bar (with ring elements) and the rotor reference axis $\alpha_{Q_{r(k)}} = \pi p / Q_r$,

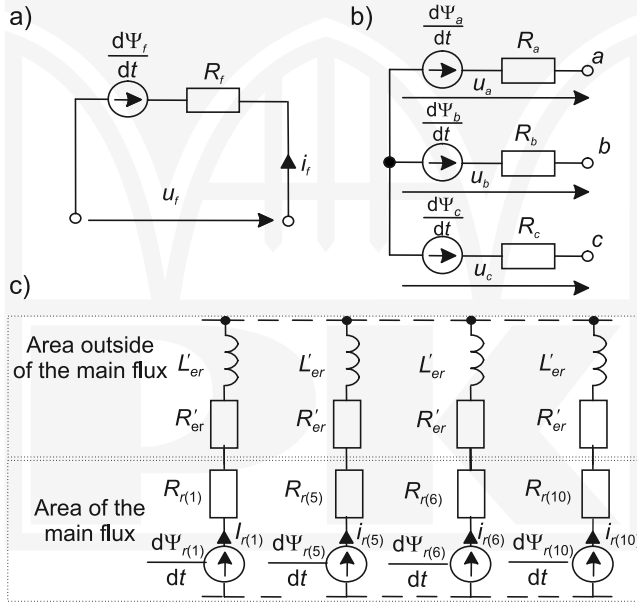Q_r –   number of damping bars per pole.

Fig. 7. Equivalent circuit parameters of a salient pole synchronous generator in the stator and rotor natural reference frame in the no-load state: a) field winding, b) stator windings, c) damping circuits reduced to single phases

As shown in [23] in the no-load steady state in the damping bars, the amplitude of higher harmonic currents $i_{r(k)v}$ are very small. So, for the non-linear model, the influence of the $i_{r(k)v}$ currents on the self and mutual inductance distributions and the field winding ampere conductors can be omitted. In the no-load steady state, it can be assumed that the self and mutual inductance distributions are dependent only on the electrical angle of the

rotor position θ and field current i_f. From the equivalent circuit of a salient pole synchronous generator (Fig. 7), the voltage u_a, u_b and u_c of induced in the three-phase armature windings, the voltage $d\Psi_{r(k)}(\theta, i_f)/dt$ induced in the the k-th damping bar (taking into account the field winding and the electrical angle of the rotor position)can be derived from the equations in stator coordinates (for the stator windings – Fig. 7) and in rotor coordinates (for the field winding and damping bars – Fig. 7)

$$\frac{d\psi_a(\theta, i_f)}{dt} = u_a, \quad \frac{d\psi_b(\theta, i_f)}{dt} = u_b, \quad \frac{d\psi_c(\theta, i_f)}{dt} = u_c \tag{10}$$

$$\frac{d\psi_f(\theta, i_f)}{dt} + R_f i_f = u_f \tag{11}$$

$$\frac{d\psi_{r(k)}(\theta, i_f)}{dt} + R_{r(k)} i_{r(k)} + L_{er} \frac{i_{r(k)}}{dt} = 0 \tag{12}$$

$$\frac{d\theta}{dt} = p\omega \quad \text{and} \quad i_{r(1)} + i_{r(2)} + \ldots + i_{r(k)} = 0 \tag{13}$$

where:

a, b, c, f	–	indexes of stator windings and field winding,
$r(k)$	–	index of k-th-damping bar,
Ψ_a, Ψ_b, Ψ_c	–	stator linkage fluxes,
u_a, u_b, u_c	–	stator phase voltages,
i_f	–	field current,
R_f	–	resistance of field winding,
$\Psi_{r(k)}$	–	k-th-damping bar linkage flux,
$R_{r(k)}$	–	resistance of the equivalent k-th-damping bars and ring elements,
$i_{r(k)}$	–	current in equivalent k-th damping bars and ring elements,
θ	–	electrical angle of the rotor position,
ω	–	electrical angular velocity.

In equations (10)–(12),the differential linkage fluxes in no-load steady state can be derived from the equations [5]:

$$\frac{d\boldsymbol{\Psi}_{sfr}(\theta, i_f)}{dt} = \frac{d\theta}{dt} \frac{\partial \mathbf{L}_{sfr}(\theta, i_f)}{\partial \theta} \mathbf{i}_{sfr} + \mathbf{L}_{sfr}(\theta, i_f) \frac{d\mathbf{i}_{sfr}}{dt} \tag{14}$$

where:

$\mathbf{i}_{sfr}$ – matrix of stator currents (i_a, i_b, i_c are equal to 0), field current and currents in equivalent k-thdamping bars and ring elements $[i_a, i_b, i_c, i_f, i_{r(1)}, \ldots, i_{r(k)}]^T$,

$\boldsymbol{\Psi}_{sfr}$ – matrix of linkage fluxes of stator windings, field winding, andequivalent k-th damping bars $[\Psi_a, \Psi_b, \Psi_c, \Psi_f, \Psi_{r(1)}, \ldots, \Psi_{r(k)}]^T$, $\boldsymbol{\Psi}_{sfr} = \mathbf{L}_{sfr} \mathbf{i}_{sfr}$,

$\mathbf{L}_{sfr}$ – matrix of self and mutual inductances of stator-to-rotor windings and damping bars (and ring elements).

The matrix $\mathbf{L}_{sfr}$ for $k = 10$ damping bars in no-load steady state can be expressed as [5]:

$$\mathbf{L}_{sfr}(\theta,i_f) = \begin{bmatrix} L_a+L_{es} & L_{ab} & L_{ac} & L_{af}(\theta,i_f) & L_{ar(1)}(\theta,i_f) & \ldots & L_{ar(10)}(\theta,i_f) \\ L_{ba} & L_b+L_{es} & L_{bc} & L_{bf}(\theta,i_f) & L_{br(1)}(\theta,i_f) & \ldots & L_{br(10)}(\theta,i_f) \\ L_{ca} & L_{cb} & L_c+L_{es} & L_{cf}(\theta,i_f) & L_{cr(1)}(\theta,i_f) & \ldots & L_{cr(10)}(\theta,i_f) \\ L_{fa}(\theta,i_f) & L_{fb}(\theta,i_f) & L_{fc}(\theta,i_f) & L_f(\theta,i_f)+L_{ef} & L_{fr(1)}(\theta,i_f) & \ldots & L_{fr(10)}(\theta,i_f) \\ L_{r(1)a}(\theta,i_f) & L_{r(1)b}(\theta,i_f) & L_{r(1)c}(\theta,i_f) & L_{r(1)f}(\theta,i_f) & L_{r(1)}(\theta,i_f)+L_{er} & \ldots & L_{r(10)}(\theta,i_f) \\ \ldots & \ldots & \ldots & \ldots & \ldots & \ldots & \ldots \\ L_{r(10)a}(\theta,i_f) & L_{r(10)b}(\theta,i_f) & L_{r(10)c}(\theta,i_f) & L_{r(10)f}(\theta,i_f) & L_{r(10,1)}(\theta,i_f) & \cdots & L_{r(10)}(\theta,i_f)+L_{er} \end{bmatrix}$$

$$(15)$$

The stator to damping bar mutual inductance distributions $L_{sr(k)}(\theta, i_f)$, $L_{r(k)s}(\theta, i_f)$, the field winding to damping bars mutual inductance distributions $L_{fr(k)}(\theta,i_f)$, $L_{r(k)f}(\theta,i_f)$, and the damping bar self inductance distributions $L_{r(k)}(\theta, i_f)$ are determined for the same core permeability which occurs in no-load state when the field winding constitutes the only magnetomotive force, whereas $s = \{a, b, c\}$. From expressions (10)–(15) and $\mathbf{L}_{sfr} = \mathbf{L}_{sfr}(\theta,i_f)$ the u_a, u_b and u_c can be expressed:

$$\begin{bmatrix} u_a \\ u_b \\ u_c \\ u_f \\ 0 \\ \ldots \\ 0 \end{bmatrix} = \left\{ \omega\frac{\partial\mathbf{L}_{sfr}(\theta,i_f)}{\partial\theta} + \begin{bmatrix} R_a & 0 & 0 & 0 & 0 & \ldots & 0 \\ 0 & R_b & 0 & 0 & 0 & \ldots & 0 \\ 0 & 0 & R_c & 0 & 0 & \ldots & 0 \\ 0 & 0 & 0 & R_f & 0 & \ldots & 0 \\ 0 & 0 & 0 & 0 & R_{r(1)} & \ldots & 0 \\ 0 & 0 & 0 & 0 & 0 & \ldots & 0 \\ 0 & 0 & 0 & 0 & 0 & \ldots & R_{r(10)} \end{bmatrix} \right\} \begin{bmatrix} 0 \\ 0 \\ 0 \\ i_f \\ i_{r(1)} \\ \ldots \\ i_{r(10)} \end{bmatrix} + \mathbf{L}_{sfr}(\theta,i_f)\frac{d}{dt}\begin{bmatrix} 0 \\ 0 \\ 0 \\ i_f \\ i_{r(1)} \\ \ldots \\ i_{r(10)} \end{bmatrix}$$

$$(16)$$

From (16) results:

$$\mathbf{u}_{sfr} = \left(\omega\frac{\partial\mathbf{L}_{sfr}(\theta,i_f)}{\partial\theta} + \mathbf{R}_{sfr} \right)\mathbf{i}_{sfr} + \mathbf{L}_{sfr}(\theta,i_f)\frac{d\mathbf{i}_{sfr}}{dt} \tag{17}$$

where:

$\mathbf{u}_{sfr}$ – matrix of induced stator phase voltages, field voltage and shorted damping bars voltages $[u_a, u_b, u_c, u_f, 0, \ldots, 0]^T$,

R_a, R_b, R_c – stator winding resistances,

$\mathbf{R}_{sfr}$ – diagonal matrix of resistance of the stator windings, the field winding, the 10 damping bars and ring elements.

From expression (16) results, that in no-load state of the synchronous generator the circuit model of the field winding and the equivalent 10 damping bars (with the ring segments) can be expressed as [5]:

$$\begin{bmatrix} u_f \\ 0 \\ \dots \\ 0 \end{bmatrix} = \left\{ \omega \frac{\partial}{\partial\theta} \begin{bmatrix} L_f(\theta,i_f)+L_{ef} & L_{fr(1)}(\theta,i_f) & \dots & L_{fr(10)}(\theta,i_f) \\ L_{r(1)f}(\theta,i_f) & L_{r(1)}(\theta,i_f)+L_{er} & \dots & L_{r(1,10)}(\theta,i_f) \\ \dots & \dots & \dots & \dots \\ L_{r(10)f}(\theta,i_f) & L_{r(1,10)}(\theta,i_f) & \dots & L_{r(10)}(\theta,i_f)+L_{er} \end{bmatrix} + \begin{bmatrix} R_f & 0 & \dots & 0 \\ 0 & R_{r(1)} & \dots & 0 \\ \dots & \dots & \dots & \dots \\ 0 & 0 & \dots & R_{r(10)} \end{bmatrix} \right\} \times$$

$$\times \begin{bmatrix} i_f \\ i_{r(1)} \\ \dots \\ i_{r(10)} \end{bmatrix} + \left[\begin{bmatrix} L_f(\theta,i_f)+L_{ef} & L_{fr(1)}(\theta,i_f) & \dots & L_{fr(10)}(\theta,i_f) \\ L_{r(1)f}(\theta,i_f) & L_{r(1)}(\theta,i_f)+L_{er} & \dots & L_{r(1,10)}(\theta,i_f) \\ \dots & \dots & \dots & \dots \\ L_{r(10)f}(\theta,i_f) & L_{r(1,10)}(\theta,i_f) & \dots & L_{r(10)}(\theta,i_f)+L_{er} \end{bmatrix} \right] \frac{d}{dt} \begin{bmatrix} i_f \\ i_{r(1)} \\ \dots \\ i_{r(10)} \end{bmatrix} \tag{18}$$

A method of determining the self and mutual inductance distributions of stator-to-rotor windings and damping bars (with ring elements) in (15)–(18) is detailed presented in [5, 7, 16, 23, 25]. Figure 8 presents the mutual inductance distributions of field winding to damping bars $L_{r(1)f} - L_{r(5)f}$ and $L_{r(1n)f} - L_{r(5n)f}$ and the derivative distributions $\partial L_{r(1)f}/\partial\theta - \partial L_{r(3)f}/\partial\theta$ and $\partial L_{r(1n)f}/\partial\theta - \partial L_{r(3n)f}/\partial\theta$ for a linear and a nonlinear magnetic circuit of the examined 5.5 kVA with the rotor without skew. The initial length of the air gap of the pole piece in the longitudinal axis of the rotor is equal to $\delta_0 = 0.55$ mm. The simulations are carried out in the FEMM program under no-load in a steady state ($I_f =$ const.).
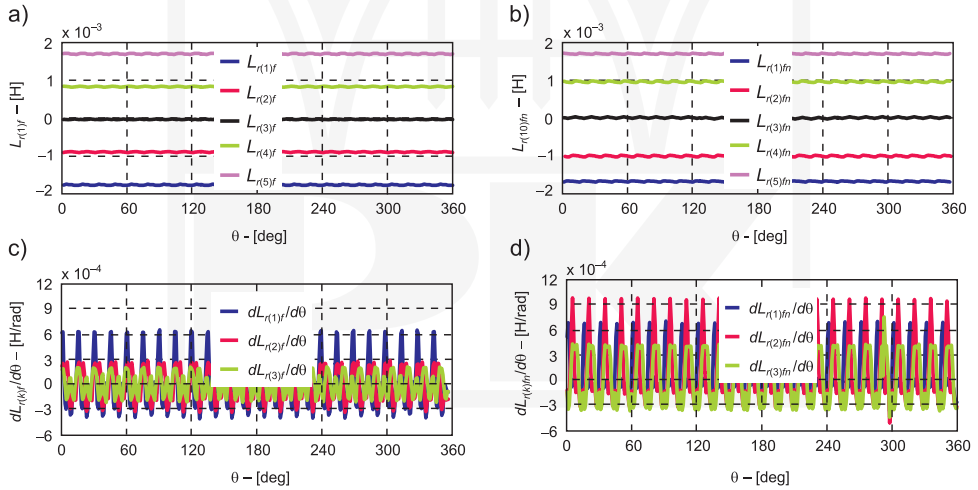

Fig. 8. Comparison of the field winding to damping bar mutual distributions without the rotor skew for linear and nonlinear model of: a) inductances $L_{r(1)f} - L_{r(5)f}$ ($L_{r(6)f} - L_{r(10)f}$), b) inductances $L_{r(1)fn} - L_{r(5)fn}$ ($L_{r(6)fn} - L_{r(10)fn}$), c) derivatives $\partial L_{r(1)f}/\partial\theta - \partial L_{r(3)f}/\partial\theta$, d) derivatives $\partial L_{r(1)fn}/\partial\theta - \partial L_{r(3)fn}/\partial\theta$

5. Experimental verification

Figure 9 shows a measurement set for the investigation of the 5.5 kVA salient pole synchronous generator with the special construction of the rotor(the additional two sets of rings connected to the 5 damping bars per pole). Experimental verification of the induced voltages in the damping bars without the rotor skew are performed under no-load of the 5.5 kVA salient pole synchronous generators. During the investigations, the damping bars were opened ($i_{r(1)} - i_{r(5)}$ were equal to zero) and the field winding was powered by a DC voltage source. The voltages in the 4 damping bars were registered using a four-channel digital oscilloscope. From (18) results that $u_{r(1)} = \omega \partial L_{r(1)fn}/\partial \theta$, $u_{r(2)} = \omega \partial L_{r(2)fn}/\partial \theta$, $u_{r(3)} = = \omega \partial L_{r(3)fn}/\partial \theta$, $u_{r(4)} = \omega \partial L_{r(4)fn}/\partial \theta$ and $u_{r(5)} = \omega \partial L_{r(5)fn}/\partial \theta$. In Figure 10, registered waveforms of $u_{r(1)}$ (Channel 1), $u_{r(2)}$ (Channel 2), $u_{r(3)}$ (Channel 3) and $u_{r(4)}$ (Channel 4) are presented.

Fig. 9. Measurement set for investigation of the induced voltages in the 5 damping bars of the 5.5 kVA salient pole synchronous generator with the special construction of the rotor
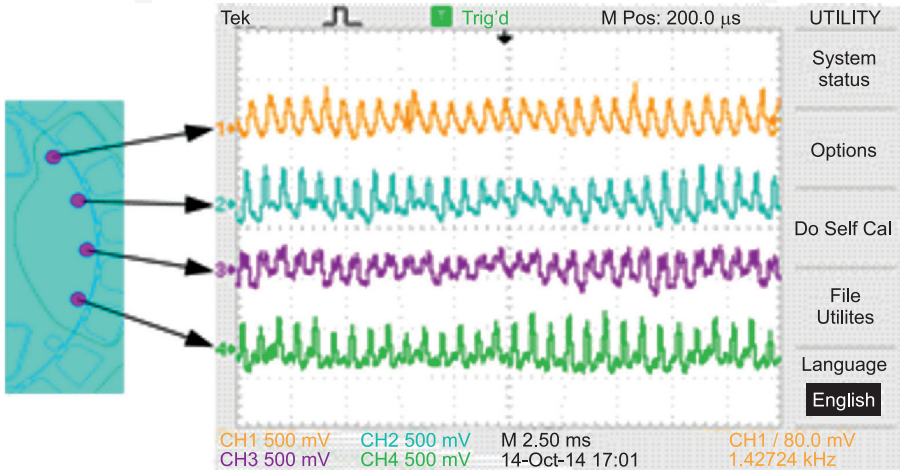

Fig. 10. Registered waveforms of the induced voltages in four damping bars under no-load conditions for the 5.5 kVA salient pole synchronous generator without the rotor skew

Registered waveforms of the induced voltages in four damping bars (Fig. 10) are very similar to the derivatives shown in Fig. 8. Deformations of the induced voltage in each damping bar result from vibrations of the rotor and the used measurement method (the induced voltages are registered between two brushes and two slip-rings).

6. Conclusion

This article presents two problems. The first is the analysis of the constant component and higher harmonic contents in the self and mutual inductance distributions in the stator natural reference frame *abc* and in the *dq*0-axes (in the rotor reference frame) for the linear and nonlinear (field) model of the salient pole synchronous generator-rated 5.5 kVA. The second problem is modeling the damping circuits on the rotor of a salient pole synchronous generator.

As shown in the paper, for the tested salient pole synchronous generator 5.5 kVA within the self and mutual stator inductance distributions, the most significant are the 2nd and 4th harmonics which are only influenced by the rotor skew to a small extent. Hence, the rotor skew on the inductance distributions in the stator natural reference frame *abc* and in the *dq*0- -axes for linear and nonlinear model have little effect.

From comparison of the linear and nonlinear model, it results that the nonlinearity slightly increases the magnitudes of 2nd harmonic. The 2nd harmonic is six times greater in mutual inductance then in the self inductance distributions. For this reason, the 2nd harmonic of the slot leakage flux introduces an alternate component that is present in the L_{d0}, L_{0d}, L_{q0} and L_{0q} mutual inductances in *dq*0-axes with and without a rotor skew.

In the second problem, this article presents the experimental verification of the proposed method of modeling the resistance and self and mutual inductance distributions of damping bars, which is detailed presented in [5]. An important advantage of this method is:

– diagonal matrix of damping bar resistances in circuital models (written as the diagonal matrix of the stator winding resistances),
– a simple way of determining the self and mutual inductance distributions both for the stator windings, field winding and *k*-th damping bars (having an even or an odd number),
– the fact that the damping bars can be treated as a single phase winding.

References

[1] Sobczyk T.J., *Methodology of mathematical modeling of induction machines* (in Polish), WNT, Warsaw 2004.
[2] Sobczyk T.J., *Extreme possibilities of circuital models of electric machines*, Electrical Power Quality and Utilisation, 2006, Vol. 7, No. 2, 103-110.
[3] Staszak J., *Modeling the electromechanical characteristics of three-phase squirrel-cage induction motor by selection the stator windings and the power supply system* (in Polish), Wydawnictwo Politechniki Świętokrzyskiej, Monograph M31, Kielce 2012.

[4] Vicol L., Banyai A., Viorel I.A., Simond J.J., *On the damper cage bars' currents calculation for salient pole large synchronous machines*, Optimization of Electrical and Electronic Equipment, 11th International Conference on 22–24 May 2008, 9-14.

[5] Ludwinek K., *Proposed way of modeling the damping circuits on the rotor of a salient pole synchronous generator* (in Polish), Zeszyty Problemowe – Maszyny Elektryczne, 2014, No. 104, Komel, Katowice, 179-186.

[6] Ludwinek K., *Model of synchronous machine for co-operation with distorted and asymmetrical electric power system* (in Polish), Zeszyty Naukowe Politechniki Świętokrzyskiej, Elektryka, 2005, No. 42, Kielce, 239-250.

[7] Ludwinek K., *Some aspects of representation of inductance distributions in dq0-axes in a salient pole synchronous generator*, Zeszyty Problemowe – Maszyny Elektryczne, 2014, No. 104, Komel, Katowice, 187-184.

[8] Zajczyk R., *Mathematical models of power system for examination of electro-mechanical unsteady states and control processes* (in Polish), Gdańsk University of Technology, Gdańsk 2003.

[9] Vermeulen H.J., Strauss J.M., Shikoana V., *Online estimation of synchronous generator parameters using PRBS perturbations*, IEEE Transactions on Power Systems, 2002, Vol. 17, No. 3, 674-700.

[10] Ludwinek K., Staszak J., *Possibility of graphical environment applications for evaluating of equivalent circuit parameters and time constants*, Przegląd Elektrotechniczny, 2011, No. 12a, 195-200.

[11] Berhausen S., Boboń A., Paszek S., *A methodology for determining electromagnetic parameters of a synchronous machine based on analysis of transient waveforms obtained by the finite element method under no-load conditions*, Zeszyty Problemowe – Maszyny Elektryczne, no. 84, 2009, published by Komel Katowice, Poland, 29-32.

[12] Berhausen S., Boboń A., *A field method for determining parameters and characteristics of a synchronous machine* (in Polish), Zeszyty Problemowe – Maszyny Elektryczne, 2011, No. 91, Komel, Katowice, 43-49.

[13] Danhong Z., *Finite element analysis of synchronous machines*, Doctor's Thesis, Pennsylvania State University, 2009.

[14] Demenko A., Pietrowski W., Stachowiak D., *Flux density calculation in permanent magnet machine using edge element method*, Przegląd Elektrotechniczny, 2005, No. 10, 2-7.

[15] Burlikowski W., *Comparison of different implementations of reluctance motor simulational model*, Proceedings of XLIII International Symposium on Electrical Machines, Poland, Poznań, 2–5 Juny, 2007, 147-150.

[16] http://www.femm.info/wiki/HomePage.

[17] Skwarczyński J., *Salient poles inner asymmetries* (in Polish), Scientific Bulletins of Stanisław Staszic Academy of Mining and Metallurgy, Electrotechnics, Bulletin 16, 1990.

[18] Tessarolo A., *Accurate Computation of Multiphase Synchronous Machine Inductances Based on Winding Function Theory*, IEEE Transactions on Energy Conversion, 2012, vol. 27, 895-904.

[19] Dąbrowski M., *Design of alternating current electrical machines* (in Polish), WNT, Warsaw 1994.

[20] Freese M., Kulig S., *Influence of constructional turbo-generator end region design on end winding inductances*, Archives of Electrical Engineering, 2012, Vol. 61, No. 2, 199-210.

[21] Paszek S., Berhausen S., Boboń A., Majka Ł., Nocoń A., Pasko M., Pruski P., Kraszewski T., *Mesurement Estimation of Dynamic Parameters of Synchronous Generators and Excitation Systems Working in the National Power System*, Monograph, Wydawnictwo Politechniki Ślaskiej, Gliwice 2013.

[22] Nadolski R., Staszak J., Harbaoui L., *Consideration of solid rotor damping circuit in natural hunting of turbogenerator*, Archives of Electrical Engineering, 1998, Vol. 47, No. 2, 233-243.

[23] Ludwinek K., *Influence of Representation of the Stator to Rotor Mutual Inductances on the Induced Phase Voltage Waveforms in a Salient Pole Synchronous Generator*, Zeszyty Problemowe – Maszyny Elektryczne, 2014, No. 104, Komel, Katowice, 147-154.

[24] Skwarczyński J., Weinreb K., *Method of Analysis of Slot Harmonics in the Salient-Pole Synchronous Generators*, International Conference on Electrical Machines (ICEM), Boston, MA, August 13–15, 1990, 1165-1170.

[25] Ludwinek K., *Representation of the stator to rotor self- and mutual inductances in a salient pole synchronous generator in the no-load state*, Zeszyty Problemowe – Maszyny Elektryczne, 2014, No. 104, Komel, Katowice, 147-154.